

Chromomagnetic dipole moments of light quarks in the bestest little Higgs model

T. Cisneros-Pérez^{1†} E. Cruz-Albaro^{2‡} A. Y. Ojeda-Castañeda^{2§} S. E. Solís-Núñez^{2¶}

¹Unidad Académica de Ciencias Químicas, Universidad Autónoma de Zacatecas, Apartado Postal C-585, 98060 Zacatecas, Mexico

²Facultad de Física, Universidad Autónoma de Zacatecas, Apartado Postal C-580, 98060 Zacatecas, Mexico

Abstract: In this study, we investigated the anomalous Chromomagnetic Dipole Moment (CMDM), denoted as $\hat{\mu}_q^{\text{BLHM}}$, of light quarks $q = (u, c, d, s, b)$ within the framework of the Bestest Little Higgs Model (BLHM) as an extension of the Standard Model (SM). Our investigation encompassed novel interactions among the light quarks, heavy quark B , and heavy bosons ($W'^{\pm}, H^{\pm}, \phi^{\pm}, \eta^{\pm}$), incorporating the extended Cabibbo-Kobayashi-Maskawa (CKM) matrix characteristic of the BLHM. We thoroughly explored the permissible parameter space, yielding a spectrum of CMDM values ranging from 10^{-10} to 10^{-3} .

Keywords: beyond standard model, flavor physics, chromomagnetic dipole, light quarks

DOI: 10.1088/1674-1137/ad62d9

I. INTRODUCTION

The CMDM of the top quark has been extensively studied theoretically within the framework of the SM [1–5], with the most accurate experimental measurement reported in [6]. Extended models in the literature have also explored both the CMDM and chromoelectric dipole moment (CEDM) [7–10], yielding results and theoretical implications that vary depending on each model beyond the SM (BSM). The prevalence of studies on the CMDM and CEDM of the top quark over the light quarks of the SM in BSM is precisely owing to the magnitude of its mass and the experimental framework in the last decade, in which interactions with heavy particles above 1 TeV were expected to be found. In this regard, we calculated the CMDMs of the light quarks and established new bounds on the parameters of the BLHM. Several experimental reports showed advances toward increasingly higher energies and hence hypothetical particles that may even exceed 5 TeV [11]. In this regard, the calculation of the CMDMs for light quarks (u, c, d, s, b) within the framework of certain BSM scenarios may seem unnecessary in the absence of experimental measurements. However, it is important to mention that a central value for $\hat{\mu}_i^{\text{SM}}$ already exists, and the CEDM is bounded. This uniquely contributes to the understanding of the BL-

HM, complementing existing studies on the subject [10, 12–14]. The CMDMs of the light quarks were calculated within the framework of the SM in [15] for spacelike value ($q^2 = -m_Z^2$), while in [16], they were obtained for timelike value ($q^2 = +m_Z^2$). In [17], the authors recalculated them for both values ($q^2 = \pm m_Z^2$), providing detailed results for the individual contributions received by each light quark from the chromodynamic and electroweak parts. A large gluon momentum transfer, $q^2 = -m_Z^2$, was used to avoid an infrared divergence in the triple gluon vertex contribution to the CMDM of the top quark [15] and because in perturbative QCD, the strong running coupling constant is found at conventional scale $\alpha_s(Q^2 = -q^2 = m_Z^2) = 0.1179$. Although α_s is in the space-like regime, its value is also used in strong interactions in the timelike domain, $q^2 > 0$ [18].

In this study, we calculated the CMDM of light quarks (u, c, d, s, b) in the BLHM (it was shown in [19] that the CEDM does not exist in this model) for both values ($q^2 = \pm m_Z^2$) of the off-shell gluon and with the on-shell quarks. In this case, we found differences in both scenarios, mainly for values greater than 2 TeV in the symmetry breaking scale of the model. The BLHM is a type-I Two Higgs Doublets Model (2HDM) that has not been explored as much as other models in the Little Higgs Model (LHM) family because it considers larger

Received 30 May 2024; Accepted 9 July 2024; Published online 10 July 2024

[†] E-mail: tzihue@gmail.com

[‡] E-mail: elicruzalbaro88@gmail.com

[§] E-mail: angelica.ojeda@fisica.uaz.edu.mx

[¶] E-mail: sara.solis@fisica.uaz.edu.mx



Content from this work may be used under the terms of the Creative Commons Attribution 3.0 licence. Any further distribution of this work must maintain attribution to the author(s) and the title of the work, journal citation and DOI. Article funded by SCOAP³ and published under licence by Chinese Physical Society and the Institute of High Energy Physics of the Chinese Academy of Sciences and the Institute of Modern Physics of the Chinese Academy of Sciences and IOP Publishing Ltd

masses whose experimental observation was more difficult. However, for the latest CERN update, we expect results from models such as BLHM to stand out. Among other objectives, the BLHM was constructed [20] to address certain issues in the LHM family such as divergent singlets, masses of heavy bosons smaller than those of heavy quarks, and custodial symmetry [21]. A unique aspect of this model is its modular structure, which requires two distinct breaking scales, f and F , under condition $F > f$. Thus, the heavy quarks depend on scale f , whereas the heavy gauge bosons depend on both f and F , where F can be as large as necessary. The BLHM also offers a highly enriched phenomenology owing to its fermionic and bosonic contents, whose contributions to the light quarks may provide interesting insight for signals of new physics in the leading medium-term planned experiments.

The rest of this paper is organized as follows. In Sec. II, we provide a brief introduction to the BLHM. In Sec. III, we discuss the effective Lagrangian containing the magnetic dipole moment form factor. In Sec. IV, we describe the parameter space of the BLHM and the experimental limits that constrain it. In Sec. V, we develop the phenomenology of the CDM of light quarks and present our results. Finally, in Sec. VI, we provide our conclusions. Appendix A details the new Feynman rules used.

II. A BRIEF REVIEW OF THE BLHM

The BLHM [20] comes from group $SO(6)_A \times SO(6)_B$, which experiences a breaking at scale f toward $SO(6)_V$ when non-linear sigma field Σ acquires a vacuum expectation value (VEV), $\langle \Sigma \rangle = 1$,

$$\Sigma = e^{i\Pi/f} e^{2i\Pi_h/f} e^{i\Pi'/f}. \quad (1)$$

This results in 15 pseudo-Nambu Goldstone bosons, parameterized through electroweak triplet ϕ^a with zero hypercharges ($a = 1, 2, 3$) and triplet η^a , where (η_1, η_2) forms a complex singlet with hypercharge, and η_3 becomes a real singlet. Scalar field σ is required to generate a collective quartic coupling [20], and $T_{L,R}^a$ denotes the generators of the $SU(2)_L$ and $SU(2)_R$ groups. Thus, we have

$$\Pi = \begin{pmatrix} \phi_a T_L^a + \eta_a T_R^a & 0 & 0 \\ 0 & 0 & i\sigma/\sqrt{2} \\ 0 & -i\sigma/\sqrt{2} & 0 \end{pmatrix}. \quad (2)$$

In matrix Π_h , $h_i^T = (h_{i1}, h_{i2}, h_{i3}, h_{i4})$, ($i = 1, 2$), represent the Higgs quadruplets of $SO(4)$,

$$\Pi_h = \begin{pmatrix} 0_{4 \times 4} & h_1 & h_2 \\ -h_1^T & 0 & 0 \\ -h_2^T & 0 & 0 \end{pmatrix}. \quad (3)$$

A. Scalar sector

In the context of the BLHM, two operators are necessary to induce the quartic coupling of the Higgs via collective symmetry breaking; none of these operators alone enables the Higgs to develop a potential:

$$\begin{aligned} P_5 &= \text{diag}(0, 0, 0, 0, 1, 0), \\ P_6 &= \text{diag}(0, 0, 0, 0, 0, 1). \end{aligned} \quad (4)$$

Thus, we can express the quartic potential as [20]

$$\begin{aligned} V_q &= \frac{1}{4} \lambda_{65} f^4 \text{Tr}(P_6 \Sigma P_5 \Sigma^T) \\ &\quad + \frac{1}{4} \lambda_{56} f^4 \text{Tr}(P_5 \Sigma P_6 \Sigma^T) \\ &= \frac{1}{4} \lambda_{65} f^4 (\Sigma_{65})^2 + \frac{1}{4} \lambda_{56} f^4 (\Sigma_{56})^2, \end{aligned} \quad (5)$$

where λ_{56} and λ_{65} are the non-zero coefficients necessary to realize collective symmetry breaking and produce a quartic coupling for the Higgs.

The initial segment of Eq. (5) induces a breaking of $SO(6)_A \times SO(6)_B$ to $SO(5)_{A5} \times SO(5)_{B6}$, whereby $SO(5)_{A5}$ prohibits h_1 from acquiring a potential, and $SO(5)_{B6}$ performs the same function for h_2 . The latter portion of Eq. (5) leads to a breaking of $SO(6)_A \times SO(6)_B$ to $SO(5)_{A6} \times SO(5)_{B5}$. If we expand Eq. (1) in powers of $1/f$ and substitute it into Eq. (5), we obtain

$$\begin{aligned} V_q &= \frac{\lambda_{65}}{2} \left(f\sigma - \frac{1}{\sqrt{2}} h_1^T h_2 + \dots \right)^2 \\ &\quad + \frac{\lambda_{56}}{2} \left(f\sigma + \frac{1}{\sqrt{2}} h_1^T h_2 + \dots \right)^2. \end{aligned} \quad (6)$$

This potential generates a mass for σ ,

$$m_\sigma^2 = (\lambda_{65} + \lambda_{56}) f^2. \quad (7)$$

According to Eq. (6), it seems that each term individually contributes to the generation of a quartic coupling for the Higgs fields. However, this effect can be nullified by redefining field σ as $\pm \frac{h_1^T h_2}{\sqrt{2}f}$, where the positive and negative signs correspond to the first and second operators in Eq. (6), respectively. In combination, however, the two expressions in Eq. (6) yield a quartic Higgs po-

tential at a tree level; this occurs after integrating σ [20–22]:

$$V_q = \frac{\lambda_{56}\lambda_{65}}{\lambda_{56} + \lambda_{65}} (h_1^T h_2)^2 = \frac{1}{2}\lambda_0 (h_1^T h_2)^2. \quad (8)$$

The expression obtained has the desired form of a collective quartic potential [20, 21]. Thus, we derive a quartic collective potential form that is dependent on two distinct couplings [20]. Note that λ_0 will be zero whenever λ_{56} and/or λ_{65} are zero. This exemplifies the concept of collective symmetry breaking.

Excluding gauge interactions, not all scalars acquire mass. Consequently, it becomes necessary to introduce the potential,

$$V_s = -\frac{f^2}{4}m_4^2 \text{Tr}(\Delta^\dagger M_{26}\Sigma M_{26}^\dagger + \Delta M_{26}\Sigma^\dagger M_{26}^\dagger) - \frac{f^2}{4}(m_5^2\Sigma_{55} + m_6^2\Sigma_{66}), \quad (9)$$

where m_4 , m_5 , and m_6 represent mass parameters, and $(\Sigma_{55}, \Sigma_{66})$ denote the matrix elements from Eq. (1). In this context, M_{26} is a matrix that contracts the $SU(2)$ indices of Δ with the $SO(6)$ indices of Σ ,

$$M_{26} = \frac{1}{\sqrt{2}} \begin{pmatrix} 0 & 0 & 1 & i & 0 & 0 \\ 1 & -i & 0 & 0 & 0 & 0 \end{pmatrix}. \quad (10)$$

Operator Δ originates from a global symmetry $SU(2)_C \times SU(2)_D$, which is spontaneously broken to diagonal $SU(2)$ at scale $F > f$ upon acquiring a VEV, $\langle \Delta \rangle = 1$. We can parameterize it in the following form:

$$\Delta = e^{2i\Pi_d/F}, \quad \Pi_d = \chi_a \frac{\tau_a}{2} \quad (a = 1, 2, 3), \quad (11)$$

where matrix Π_d incorporates the scalars of triplet χ_a , which undergo mixing with triplet ϕ_a ; τ_a denotes the Pauli matrices. Δ is linked to Σ in a manner such that the diagonal subgroup of $SU(2)_A \times SU(2)_B \subset SO(6)_A \times SO(6)_B$ is recognized as the SM $SU(2)_L$ group. If we expand operator Δ in the powers of $1/F$ and substitute it in Eq. (9), we obtain

$$V_s = \frac{1}{2}(m_\phi^2\phi_a^2 + m_\eta^2\eta_a^2 + m_1^2 h_1^T h_1 + m_2^2 h_2^T h_2), \quad (12)$$

where

$$m_\phi^2 = m_\eta^2 = m_4^2, \quad m_1^2 = \frac{1}{2}(m_4^2 + m_5^2), \quad m_2^2 = \frac{1}{2}(m_4^2 + m_6^2). \quad (13)$$

To trigger EWSB, the next potential term is introduced [20]:

$$V_{B_\mu} = m_{56}^2 f^2 \Sigma_{56} + m_{65}^2 f^2 \Sigma_{65}, \quad (14)$$

where m_{56} and m_{65} are the mass terms that correspond to matrix elements Σ_{56} and Σ_{65} , respectively. Finally, we have the complete scalar potential,

$$V = V_q + V_s + V_{B_\mu}. \quad (15)$$

A potential for the Higgs doublets is necessary; hence, we minimize Eq. (15) with respect to σ and then substitute the resulting expression back in Eq. (15), yielding the following expression:

$$V_H = \frac{1}{2} [m_1^2 h_1^T h_1 + m_2^2 h_2^T h_2 - 2B_\mu h_1^T h_2 + \lambda_0 (h_1^T h_2)^2], \quad (16)$$

where

$$B_\mu = 2 \frac{\lambda_{56}m_{65}^2 + \lambda_{65}m_{56}^2}{\lambda_{56} + \lambda_{65}}. \quad (17)$$

The potential given by Eq. (16) reaches a minimum when $m_1 m_2 > 0$, and EWSB necessitates that $B_\mu > m_1 m_2$. Note that term B_μ vanishes if either $\lambda_{56} = 0$, $\lambda_{65} = 0$, or both are zero in Eq. (17). Following EWSB, the Higgs doublets acquire VEVs given by

$$\langle h_1 \rangle = v_1, \quad \langle h_2 \rangle = v_2. \quad (18)$$

The two terms in Eq. (18) are required to minimize Eq. (16), leading to the following relationships:

$$v_1^2 = \frac{1}{\lambda_0} \frac{m_2}{m_1} (B_\mu - m_1 m_2), \quad (19)$$

$$v_2^2 = \frac{1}{\lambda_0} \frac{m_1}{m_2} (B_\mu - m_1 m_2), \quad (20)$$

where the β angle between v_1 and v_2 [20] fulfills the expression

$$\tan\beta = \frac{\langle h_{11} \rangle}{\langle h_{21} \rangle} = \frac{v_1}{v_2} = \frac{m_2}{m_1}, \quad (21)$$

and we thus have that

$$v^2 = v_1^2 + v_2^2 = \frac{1}{\lambda_0} \left(\frac{m_1^2 + m_2^2}{m_1 m_2} \right) (B_\mu - m_1 m_2) \simeq (246 \text{ GeV})^2. \quad (22)$$

Following EWSB, the scalar sector [20, 22] gives rise to massive states such as h^0 (the SM Higgs), A^0 , H^\pm , and H^0 , each having their respective masses:

$$m_{G^0}^2 = m_{G^\pm}^2 = 0, \quad (23)$$

$$m_{A^0}^2 = m_{H^\pm}^2 = m_1^2 + m_2^2, \quad (24)$$

$$m_{h^0, H^0}^2 = \frac{B_\mu}{\sin 2\beta} \mp \sqrt{\frac{B_\mu^2}{\sin^2 2\beta} - 2\lambda_0\beta_\mu v^2 \sin 2\beta + \lambda_0^2 v^4 \sin^2 2\beta}, \quad (25)$$

where G^0 and G^\pm represent the Goldstone bosons that are absorbed to confer masses to the W^\pm and Z bosons of the SM.

B. Gauge boson sector

The Lagrangian including the gauge kinetic terms is given by [20, 22]

$$\mathcal{L} = \frac{f^2}{8} \text{Tr} (D_\mu \Sigma^\dagger D^\mu \Sigma) + \frac{F^2}{4} \text{Tr} (D_\mu \Delta^\dagger D^\mu \Delta), \quad (26)$$

where $D_\mu \Sigma$ and $D_\mu \Delta$ are the covariant derivatives,

$$D_\mu \Sigma = i \sum_a (g_A A_{1\mu}^a T_L^a \Sigma - g_B A_{2\mu}^a \Sigma T_L^a) + i g' B_3 (T_R^3 \Sigma - \Sigma T_R^3), \quad (27)$$

$$D_\mu \Delta = \frac{i}{2} \sum_a (g_A A_{1\mu}^a \tau_a \Delta - g_B A_{2\mu}^a \Delta \tau_a), \quad (28)$$

where $(A_{1\mu}^a, A_{2\mu}^a)$ represent the eigenstates of the gauge bosons, g' is the coupling constant of $U(1)_Y$, and g is the coupling constant of $SU(2)_L$. These terms are related to couplings g_A and g_B of $SU(2)_A \times SU(2)_B$ as follows:

$$g = \frac{g_A g_B}{\sqrt{g_A^2 + g_B^2}}, \quad (29)$$

$$s_g = \sin \theta_g = \frac{g_A}{\sqrt{g_A^2 + g_B^2}}, \quad (30)$$

$$c_g = \cos \theta_g = \frac{g_B}{\sqrt{g_A^2 + g_B^2}}, \quad (31)$$

where θ_g is the mixing angle; if $g_A = g_B$, then $\tan \theta_g = 1$.

In the context of the BLHM, the masses of both heavy gauge bosons W'^\pm , Z' , and those of the SM bosons are

also generated from [20, 22]

$$m_{Z'}^2 = \frac{1}{4}(g_A^2 + g_B^2)(f^2 + F^2) - \frac{1}{4}g^2 v^2 + \left(2g^2 + \frac{3f^2}{f^2 + F^2} \times (g^2 + g'^2)(s_g^2 - c_g^2)\right) \frac{v^4}{48f^2}, \quad (32)$$

$$m_{W'}^2 = \frac{1}{4}(g_A^2 + g_B^2)(f^2 + F^2) - m_W^2. \quad (33)$$

C. Fermion sector

The Lagrangian that governs the fermion sector of the BLHM is given by [20]

$$\mathcal{L}_f = y_1 f Q^T S \Sigma S U^c + y_2 f Q_a^T \Sigma U^c + y_3 f Q^T \Sigma U_5^c + y_b f q_3^T (-2iT_R^3 \Sigma) U_b^c + \text{h.c.}, \quad (34)$$

where (Q, Q') and (U, U') are the multiplets of $SO(6)_A$ and $SO(6)_B$, respectively, defined by

$$Q^T = \frac{1}{\sqrt{2}} \left[-(Q_{a1} + Q_{b2}), i(Q_{a1} - Q_{b2}), (Q_{a2} - Q_{b1}), i(Q_{a2} + Q_{b1}), Q_5, Q_6 \right], \quad (35)$$

where (Q_{a1}, Q_{a2}) and (Q_{b1}, Q_{b2}) represent the $SU(2)_L$ doublets, and (Q_5, Q_6) are the singlets under $SU(2)_L \times SU(2)_R = SO(4)$. Meanwhile,

$$(U^c)^T = \frac{1}{\sqrt{2}} \left[-(U_{b1}^c + U_{a2}^c), i(U_{b1}^c - U_{a2}^c), (U_{b2}^c - U_{a1}^c), i(U_{b2}^c + U_{a1}^c), U_5^c, U_6^c \right], \quad (36)$$

where $(U_{a2}^c, -U_{a1}^c)$ and $(-U_{b2}^c, U_{b1}^c)$ represent the doublets of $SU(2)_L$ along with singlets (U_5, U_6) . In addition,

$$Q_a^T = \frac{1}{\sqrt{2}} (-Q'_{a1}, iQ'_{a1}, Q'_{a2}, iQ'_{a2}, 0, 0) \quad (37)$$

$$U_5^{cT} = (0, 0, 0, 0, U_5^c, 0), \quad (38)$$

are a doublet of $SU(2)_A$ and singlet of $SU(2)_{A,B}$, respectively. $S = \text{diag}(1, 1, 1, 1, -1, -1)$ represents a symmetry operator, (y_1, y_2, y_3) denote the Yukawa couplings, and term (q_3, U_b^c) in Eq. (34) encodes information regarding the bottom quark. The BLHM introduces novel physics into the gauge, fermion, and Higgs sectors, leading to the presence of partner particles for the majority of SM particles. Given that top quark loops contribute signific-

antly to the divergent quantum corrections of the Higgs mass in the SM, the new heavy quarks introduced in the BLHM framework are expected to play a pivotal role in addressing the hierarchy problem. The heavy quarks include T , T^5 , T^6 , $T^{2/3}$, $T^{5/3}$, and B , each having the following assigned masses [20]:

$$m_T^2 = (y_1^2 + y_2^2)f^2 + \frac{9y_1^2y_2^2y_3^2}{(y_1^2 + y_2^2)(y_2^2 - y_3^2)}, \quad (39)$$

$$m_{T^5}^2 = (y_1^2 + y_3^2)f^2 - \frac{9y_1^2y_2^2y_3^2}{(y_1^2 + y_3^2)(y_2^2 - y_3^2)}, \quad (40)$$

$$m_{T^6}^2 = m_{T^{2/3}}^2 = m_{T^{5/3}}^2 = y_1^2 f^2, \quad (41)$$

$$m_B^2 = y_B^2 f^2 = (y_1^2 + y_2^2)f^2. \quad (42)$$

In the Lagrangian of the quark sector [20], the Yukawa couplings are constrained to $0 < y_i < 1$. Additionally, the masses of the top (t) and bottom (b) quarks are generated by Yukawa couplings y_t and y_b [22] as follows:

$$m_t^2 = y_t^2 v_1^2, \quad (43)$$

$$m_b^2 = y_b^2 v_1^2 - \frac{2y_b^2}{3 \sin^2 \beta} \frac{v_1^4}{f^2}. \quad (44)$$

Coupling y_t , given by

$$y_t^2 = \frac{9y_1^2y_2^2y_3^2}{(y_1^2 + y_2^2)(y_1^2 + y_3^2)}, \quad (45)$$

is a part of the measure of fine-tuning in the BLHM [22], defined as

$$\Psi = \frac{27f^2}{8\pi^2 v^2 \lambda_0 \cos^2 \beta} \frac{|y_1|^2 |y_2|^2 |y_3|^2}{|y_2|^2 - |y_3|^2} \log \frac{|y_1|^2 + |y_2|^2}{|y_1|^2 + |y_3|^2}. \quad (46)$$

In this study, we implemented a parameter space in which angle β assumes the role of most important free parameter. Given that Eq. (46) also depends on β , it is essential to keep its values bounded, that is, $\Psi \leq 2$, to avoid model fine-tuning [20].

D. Flavor mixing in the BLHM

In the original development of the BLHM [20], the authors did not include interactions between heavy quarks ($T, T^5, T^6, T^{2/3}, T^{5/3}, B$) and light quarks of the SM (u, c, d, s). This omission prevents the calculation of observables such as the one proposed in this study. Therefore, we implemented the extension to the BLHM introduced in [19]. This extension allowed us to obtain inter-

actions and contributions from heavy quarks to the chromodipole moments of light quarks. The best approach to perform this is by adding terms

$$y_B f q_1 (-2iT_R^2 \Sigma) d_B^c, \quad y_B f q_2 (-2iT_R^2 \Sigma) d_B^c, \quad (47)$$

to the Lagrangian expressed by Eq. (34). Here, $y_B^2 = y_1^2 + y_2^2$ is the Yukawa coupling of the heavy B quark, q_1 and q_2 are the multiplets of the light SM quarks, and d_B^c is a new multiplet containing the heavy B quark. This modification leads to the interactions among scalar fields ($H^\pm, \phi^\pm, \eta^\pm$), heavy quark B , and light SM quarks (u, c, d, s). The vectorial interactions among fields (W^\pm, W'^\pm), heavy quark B , and light SM quarks are allowed by adding the following terms to the Lagrangian that describes the fermion-gauge interactions [20, 22]:

$$\sum_{i=1}^2 i \bar{\sigma}_\mu Q_3^\dagger D^\mu q_i, \quad \sum_{i=1}^4 i \bar{\sigma}_\mu q_i^\dagger D^\mu U^c, \quad (48)$$

where $\bar{\sigma}_\mu = -\sigma_\mu$ are the Pauli matrices, $Q_3^T = (1/\sqrt{2})(0, 0, B, iB, 0, 0)$, and $q_i^{T'} = (0, 0, 0, 0, q_i^c, 0)$ with $i = 1, 2$. Covariant derivative D_μ contains information about (W^\pm, W'^\pm). With these changes, we can introduce two extended matrices of the Cabibbo-Kobayashi-Maskawa (CKM) type [23], V_{Hu} and V_{Hd} , such that $V_{\text{CKM}} = V_{Hu}^\dagger V_{Hd}$, where V_{CKM} is the CKM matrix of the SM. Regarding the interactions of light quarks with the neutral heavy bosons ($h^0, H^0, A^0, \phi^0, \eta^0, \sigma, Z, Z', \gamma$) and quark B , they are also included in Eqs. (47) and (48).

III. THE CMDM IN THE BLHM

The effective Lagrangian describing the contributions of vertex $g \bar{q}_i q_i$, where $q_i = u, c, d, s$, is expressed as

$$\mathcal{L}_{\text{eff}} = -\frac{1}{2} \bar{q}_i T_a \sigma^{\mu\nu} (\hat{\mu}_{q_i} + i \hat{d}_{q_i} \gamma^5) q_i G_{\mu\nu}^a, \quad (49)$$

where $G_{\mu\nu}^a$ represents the gluon field strength tensor, T_a denotes the colour generators of $SU(3)_C$, $\hat{\mu}_{q_i}$ denotes the CMDM, and \hat{d}_{q_i} represents the CEDM, such that

$$\hat{\mu}_{q_i} = \frac{m_{q_i}}{g_s} \mu_{q_i}, \quad \hat{d}_{q_i} = \frac{m_{q_i}}{g_s} d_{q_i}. \quad (50)$$

The definitions provided by Eq. (50) are the standard relations for the CMDM and CEDM commonly found in the literature, given that \mathcal{L}_{eff} has dimension 5. Here, m_{q_i} denotes the mass of each light quark and $g_s = \sqrt{4\pi\alpha_s}$ represents the coupling constant of the group. In our scenario, we solely need to evaluate chromomagnetic form factor μ_{q_i} originating from one-loop contributions of scal-

ar fields $A^0, H^0, H^\pm, h^0, \sigma, \phi^0, \phi^\pm, \eta^0, \eta^\pm$, vector fields Z^0, Z', W^\pm, W'^\pm , and heavy quarks $T, T^5, T^6, T^{2/3}, T^{5/3}, B$. Concerning the CEDM, it was demonstrated [5] to be identically zero within the BLHM framework, thus necessitating no further consideration in this study.

IV. PARAMETER SPACE OF THE BLHM

Two types of parameter spaces have been utilized in the different studies on the BLHM. The initial studies on the model [22, 24–26] parameterized Yukawa couplings (y_1, y_2, y_3) in terms of two angles $(\theta_{12}, \theta_{13})$ that divide the space into two parts, leading to heavy quark masses that acquire two hierarchies depending on whether $y_2 < y_3$ or $y_3 < y_2$. By contrast, the parameter space employed in this study is the same as that proposed in [5, 19, 27]. It can be optimized more easily without dividing it into two parts or inducing hierarchies in the masses of heavy quarks. In this implementation, the Yukawa couplings of the BLHM are maintained in the range $0 < y_i < 1$, ensuring that the relation given by Eq. (45) is satisfied under the condition given by Eq. (43) and value $m_t = 172.13$ GeV [28]. We solved Eq. (25) to deduce the masses of the scalar bosons in the model considering $0.15 \leq \beta \leq 1.49$ radians and $m_{H^0} = 125.46$ GeV [29] under condition $\lambda^0 < 4\pi$ [26]. The authors of the BLHM imposed condition $\tan\beta > 1$, thereby ensuring that the contributions from radiative corrections at one-loop from the top quark and heavy tops to the Higgs mass are minimized. This narrows down the interval for β to $0.79 < \beta < 1.49$ radians. According to the constraints deduced in [27] to maintain fine-tuning Ψ (Eq. (46)) within interval $0 < \Psi < 2$, we also adopted the same values for all parameters of the BLHM, as shown in Table 1. This table is divided into minima and maxima according to the different intervals of breaking scale f ; note the allowed masses for scalar fields A^0, H^0 , and H^\pm . Parameter α is the mixing angle between fields h^0 and H^0 [22], such that the alignment limit is satisfied, $\cos(\beta - \alpha) \approx 0$ [30]. The mass of scalar boson σ is the largest among those of the scalars of the BLHM and is given as $m_\sigma^2 = 2\lambda^0 K_\sigma f^2$ [26], which is equivalent to Eq. (7) but more easy to calculate. For scalar $\eta^0 = m_4$, where

m_4 is a free parameter of the model [20], we set the $30 \leq m_4 \leq 800$ GeV range [19] owing to the growing magnitudes of masses for experimentally sought new particles. In the case of charged scalar bosons ϕ^\pm, η^\pm and neutral ϕ^0 , their masses also depend on m_4 as well as both breaking scales, f and F , and one-loop contributions from the Coleman-Weinberg potential [20, 24]. Note that $1 \leq f \leq 3$ TeV and $F = 5$ TeV in Table 2.

The masses of heavy vector bosons (W'^\pm, Z') depend on scales f and $F = 5$ TeV. To determine their masses, we used Eqs. (32) and (33). The results are shown in Table 3.

The masses of the six heavy quarks introduced in this model are given by Eqs. (39)–(42), in which we do not observe a dependence on angle β but only on Yukawa couplings (y_1, y_2, y_3) and breaking scale f . This allows for simpler calculation of these masses in the $1 < f < 3$ TeV interval; their values are shown in Table 4.

A. Experimental limits for the BLHM

Experimentally, the pursuit of a heavy neutral scalar, such as A^0 and H^0 , is in line with the mass range of the BLHM. In [31], masses in the range of 230–800 GeV for m_{A^0} and 130–700 GeV for m_{H^0} were explored in decay $A \rightarrow ZH$, based on an integrated luminosity of 139 fb^{-1} from pp collisions at $\sqrt{s} = 13$ TeV recorded by the ATLAS detector and interpreted within the 2HDM framework. A study based on ATLAS data [32] analyzed process $A \rightarrow Zh$ excluding masses of A^0 below 1 TeV at 95% C.L. for all types of 2HDM. Similarly, in [33], based on CMS data, masses of A^0 below 1 TeV were also ruled out. In [34], type-I 2HDMs were investigated through the simulation of process $e^-e^+ \rightarrow AH$ using the SiD detector at the ILC, with an integrated luminosity of 500 fb^{-1} . This resulted in ranges of $200 < m_{A^0} < 250$ GeV and $150 < m_{H^0} < 250$ GeV. For H^\pm , a study [35] examined process $H^\pm \rightarrow HW^\pm$ at CMS in pp collisions at $\sqrt{s} = 13$ TeV with an integrated luminosity of 138 fb^{-1} , considering m_{H^\pm} in the range of 300–700 GeV. Additionally, in [6], decay $H^+ \rightarrow t\bar{b}$ was explored in pp collisions at $\sqrt{s} = 13$ TeV using 139 fb^{-1} of data from ATLAS, with m_{H^+} considered in the range of 200–2000 GeV. The ex-

Table 1. Parameters and scalar masses constrained in the BLHM.

Parameter	$f(1 \text{ TeV})$		$f(2 \text{ TeV})$		$f(3 \text{ TeV})$		Unit
	Min	Max	Min	Max	Min	Max	
β	0.79	1.47	0.79	1.36	0.79	1.24	rad
α	−0.99	0.00	−0.99	−0.16	−0.99	−0.31	rad
Ψ	0.096	2.11	0.38	2.03	0.87	2.04	–
m_{A^0}	125.0	884.86	125.0	322.75	125.0	207.07	GeV
m_{H^0}	872.04	1236.06	872.04	921.42	872.04	887.53	GeV
m_{H^\pm}	125.0	884.86	125.0	322.75	125.0	207.07	GeV

Table 2. Scalar masses of the BLHM.

Mass	Values		Unit
	$f(1\text{ TeV})$	$f(3\text{ TeV})$	
m_σ	1414.2	4242.6	GeV
m_{ϕ^0}	836.1	999.3	GeV
m_{ϕ^\pm}	841.9	1031.9	GeV
m_{η^\pm}	580.0	1013.9	GeV

Table 3. Vector masses of the BLHM.

Mass	Values		Unit
	$f(1\text{ TeV})$	$f(3\text{ TeV})$	
$m_{W'^\pm}$	3328.63	3806.44	GeV
$m_{Z'}$	3327.65	3805.58	GeV

Table 4. Quark masses of the BLHM.

Mass	$1 \leq f \leq 3\text{ TeV}$		Unit
	Min	Max	
m_T	1140.18	3420.53	GeV
m_{T^5}	773.88	2321.66	GeV
m_{T^6}	780.0	2100.0	GeV
$m_{T^{2/3}}$	780.0	2100.0	GeV
$m_{T^{5/3}}$	780.0	2100.0	GeV
m_B	1140.18	3420.53	GeV

ploration for heavy Higgs bosons seems to be highly active in various channels and theoretical frameworks, such as 2HDM. Furthermore, all the mass ranges either encompass or are encompassed by those investigated in this study.

The presence of neutral and charged fields, denoted by (ϕ, η) , derived from pseudo Goldstone bosons, is a common feature shared with other LHM frameworks and proposals for dark matter. However, experimental searches primarily focus on fields associated with the Higgs rather than scalars of this nature [36–38]. Another distinctive characteristic of the BLHM is real scalar field σ , which is anticipated to be the heaviest among the scalars. Nevertheless, its contribution to the CMDM of light SM quarks is nearly negligible owing to certain constraints imposed by the CKM extended matrix. Within the domain of heavy quarks, decay channels $T \rightarrow Ht$ or $T \rightarrow Zt$ were examined in [39]. This study analyzed proton-proton collisions at $\sqrt{s} = 13\text{ TeV}$ with an integrated luminosity of 139 fb^{-1} at ATLAS, revealing no significant signals at the 95% confidence level for the mass of T in the range of 1.6–2.3 TeV. Similar searches for T and B were reported in [40–42]. In [40], the authors also explored the potential decay of quarks with charge $5/3$,

such as $T^{5/3}$, to Wt , establishing a lower limit for $m_{T^{5/3}}$ of 1.42 TeV. For the BLHM within our parameter space, we found that $m_{T^{5/3}} = m_{T^6} = m_{T^{2/3}}$ span the range of 780–2100 GeV, as shown in Table 4. In the BLHM, we introduced additional vector bosons W'^\pm and Z' , whose masses were constrained to be equal based on the properties chosen for our parameter space. Several investigations on the existence of the W' boson have been reported. In [43], various mass ranges for $m_{W'}$ were considered within the theoretical framework of different extended models, with values ranging from 2.2 to 4.8 TeV. Regarding the Z' boson, recent searches indicate that its mass exceeds 4.7 TeV [44] and is within the range of 800–3700 GeV [45].

V. PHENOMENOLOGY OF THE CMDM OF THE LIGHT QUARKS

Regarding the CMDM, the permissible one-loop diagrams involving scalar and vector contributions are shown in Fig. 1. The amplitudes associated with the dipole diagrams for each of the (u, c, d, s, b) quarks are as follows:

$$\begin{aligned}
\mathcal{M}_{q_n}^\mu(S) &= \sum_{i,j} \int \frac{d^4k}{(2\pi)^4} \bar{u}_n(p') (S_{nj}^* + P_{nj}^* \gamma^5) \delta_{A\alpha_1} \\
&\times \left[i \frac{k + \not{p}' + m_{Q_j}}{(k+p')^2 - m_{Q_j}^2} \delta_{\alpha_1\alpha_3} \right] (-ig_s \gamma^\mu T_{\alpha_2\alpha_3}^a) \\
&\times \left[i \frac{\not{k} + \not{p} + m_{Q_j}}{(k+p)^2 - m_{Q_j}^2} \right] (S_{nj} + P_{nj} \gamma^5) \delta_{B\alpha_4} u_n(p) \\
&\times \left(\frac{i}{k^2 - m_{S_i}^2} \right) V_{H_j q_n}^* V_{H_j q_n} \quad (51)
\end{aligned}$$

and

$$\begin{aligned}
\mathcal{M}_{q_n}^\mu(V) &= \sum_{i,j} \int \frac{d^4k}{(2\pi)^4} \bar{u}_n(p') \gamma^{\alpha_1} (V_{nj}^* + A_{nj}^* \gamma^5) \delta_{A\alpha_1} \\
&\times \left[i \frac{\not{k} + \not{p}' + m_{Q_j}}{(k+p')^2 - m_{Q_j}^2} \delta_{\alpha_1\alpha_3} \right] (-ig_s \gamma^\mu T_{\alpha_2\alpha_3}^a) \\
&\times \left[i \frac{\not{k} + \not{p} + m_{Q_j}}{(k+p)^2 - m_{Q_j}^2} \right] \gamma^{\alpha_2} (V_{nj} + A_{nj} \gamma^5) \delta_{B\alpha_4} u_n(p) \\
&\times \left[\frac{i}{k^2 - m_{V_i}^2} \left(-g_{\alpha_1\alpha_2} + \frac{k_{\alpha_1} k_{\alpha_2}}{m_{V_i}^2} \right) \right] V_{H_j q_n}^* V_{H_j q_n}, \quad (52)
\end{aligned}$$

where $T_{\alpha_n\alpha_m}^a$ represents the generators of $SU(3)$. Coefficients $(S_{nj}, P_{nj}, V_{nj}, A_{nj})$ encompass all contributions from the BLHM, quantified by vertices $\bar{Q}_j S_i q_n$, $\bar{q}_n S_i^\dagger Q_j$ for scalar and pseudoscalar interactions, and $\bar{Q}_j V_i q_n$, $\bar{q}_n V_i^\dagger Q_j$ for vector and axial interactions, respectively. Matrix ele-

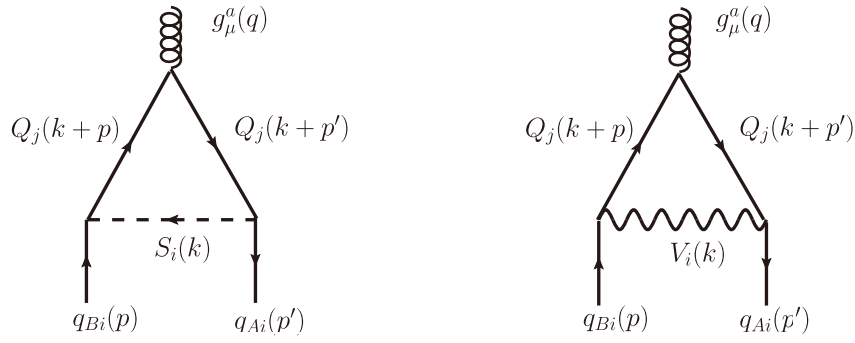


Fig. 1. Left: interactions of SM light quarks (u, c, d, s, b) and BLHM heavy quarks $Q = (T, T^5, T^6, T^{2/3}, T^{5/3}, B)$ with scalar fields S_i : $A^0, H^0, h^0, H^\pm, \phi^0, \eta^0, \sigma, \phi^\pm, \eta^\pm$. Right: interactions of the same quarks with vector fields V_i : $Z^0, W^\pm, \gamma, Z', W'^\pm$.

ments $V_{H_j q_n}^* V_{H_j q_n}$ pertain to the extended CKM matrix. The amplitudes given by Eqs. (51) and (52) were computed utilizing the FeynCalc package [46] and Package X [47] available in Mathematica.

In interactions involving charged bosons, both scalar and vector, the extended CKM matrix for the BLHM, denoted as $V_{\text{CKM}} = V_{Hu}^\dagger V_{Hd}$ and introduced in [19], must be taken into account. Here, unitary matrix V_{Hu}^\dagger represents transitions from heavy quarks to light up-type quarks, while V_{Hd} represents transitions from heavy quarks to light down-type quarks. The CKM extended matrix can be conceptualized as the product of three rotation matrices [48, 49],

$$\begin{aligned}
 V_{Hd} &= \begin{pmatrix} 1 & 0 & 0 \\ 0 & c_{23}^d & s_{23}^d e^{-i\delta_{23}^d} \\ 0 & -s_{23}^d e^{i\delta_{23}^d} & c_{23}^d \end{pmatrix} \\
 &\times \begin{pmatrix} c_{13}^d & 0 & s_{13}^d e^{-i\delta_{13}^d} \\ 0 & 1 & 0 \\ -s_{13}^d e^{i\delta_{13}^d} & 0 & c_{13}^d \end{pmatrix} \\
 &\times \begin{pmatrix} c_{12}^d & s_{12}^d e^{-i\delta_{12}^d} & 0 \\ -s_{12}^d e^{i\delta_{12}^d} & c_{12}^d & 0 \\ 0 & 0 & 1 \end{pmatrix}, \quad (53)
 \end{aligned}$$

where parameters c_{ij}^d and s_{ij}^d are expressed in relation to angles $(\theta_{12}, \theta_{23}, \theta_{13})$ and phases $(\delta_{12}, \delta_{23}, \delta_{13})$.

In [19] and [27], the authors chose three cases to parameterize matrices V_{Hu} and V_{Hd} in such a way that results with greater variation could be obtained. However, in [27], the authors mostly found the same behavior for the three cases of the extended CKM matrices. For this reason, in this study, we chose to use only the third case, given that we also calculated the CMDM.

We constructed the extended CKM matrix by first substituting values $s_{23}^d = 1/\sqrt{2}$, $s_{12}^d = s_{13}^d = 0$, $\delta_{12}^d = \delta_{23}^d = \delta_{13}^d = 0$ into matrix V_{Hd} in Eq. (53), obtaining matrix

$$V_{Hd} = \begin{pmatrix} 1 & 0 & 0 \\ 0 & 1/\sqrt{2} & 1/\sqrt{2} \\ 0 & -1/\sqrt{2} & 1/\sqrt{2} \end{pmatrix}, \quad (54)$$

and through product $(V_{Hd}^\dagger)^{-1} V_{\text{CKM}}^\dagger$, obtaining matrix

$$V_{Hu} = \begin{pmatrix} 0.973 & 0.221 & 0.008 \\ 0.160 & 0.692 & 0.746 \\ -0.156 & -0.686 & 0.687 \end{pmatrix}. \quad (55)$$

According to the experimental values of the CKM matrix of the SM and the properties of unitarity, the following relations between its rows hold, and similar ones hold for the columns:

$$\begin{aligned}
 \sum_{i=1}^3 |V_{ui}|^2 - 1 &= -0.0004 \pm 0.0007 \\
 \sum_{i=1}^3 |V_{ci}|^2 - 1 &= +0.11 \pm 0.08 \\
 \sum_{i=1}^3 |V_{ti}|^2 - 1 &= +0.00 \pm 0.2
 \end{aligned} \quad (56)$$

Similarly, the unitarity conditions for the matrix expressed by Eq. (55) are satisfied:

$$\begin{aligned}
 \sum_{i=1}^3 |V_{Hu_{1i}}|^2 - 1 &= -0.002 \pm 0.0002 \\
 \sum_{i=1}^3 |V_{Hu_{2i}}|^2 - 1 &= +0.062 \pm 0.03 \\
 \sum_{i=1}^3 |V_{Hu_{3i}}|^2 - 1 &= -0.031 \pm 0.004
 \end{aligned} \quad (57)$$

Based on relation $V_{\text{CKM}} = V_{Hu}^\dagger V_{Hd}$, the existence of a

certain level of congruence between V_{Hu} in Eq. (55) and the V_{CKM} matrix is natural. However, note from Eqs. (56) and (57) that the flavor constraints are less strict than those found in the V_{CKM} matrix. Similarly, when the GIM mechanism is applied in the SM, significant suppressions are expected for processes such as rare decays; this does not happen with the extended CKM matrices in the BLHM [19].

A. Results

We computed the CMDMs of light quarks (u, c, d, s, b) under one-loop contributions from heavy quarks and bosons in the BLHM. We also included interactions with fields (h^0, Z, γ, W^\pm) of the SM. Interactions with charged bosons ($W^\pm, W'^\pm, H^\pm, \phi^\pm, \eta^\pm$) were mediated by the matrix elements of V_{Hu} and V_{Hd} , that is, Eqs. (55) and (54), respectively. Given that the virtual quarks in the dipole could only be the quarks from the BLHM, certain constraints emerged for the contributions of the model toward the light quarks of the SM. One of them arose with the charged bosons because in most valid vertices, only interactions with heavy quark B occurred (see Tables 12 and 13 in Appendix A). Although heavy quarks ($T, T^5, T^6, T^{2/3}, T^{5/3}$) do not interact with light quarks (u, c, d, s), the contributions from the BLHM, because of the interactions with fields ($H^0, A^0, \phi^0, \eta^0, \sigma, Z'$), enhance their CMDMs in relation to those of the SM. We evaluated the CMDM of the light quarks taking gluon off-shell ($q^2 \neq 0$) in two scenarios: spacelike ($q^2 = -m_Z^2$) and timelike ($q^2 = m_Z^2$). By solving the amplitudes given by Eqs. (51) and (52), the expressions of the magnetic form factor in terms of the Passarino-Veltman functions of type A_0 , B_0 , and C_0 were obtained.

Figures 2 and 3 show the CMDM plots of the up and charm quarks. Owing to the BLHM contributions to the dipoles of these two quarks having similar magnitudes, $O(10^{-8})$, we plot them together for $\beta = (0.79, 1.24, 1.49)$ radians. It is important to note that they only received contributions from the B quark, both with charged and

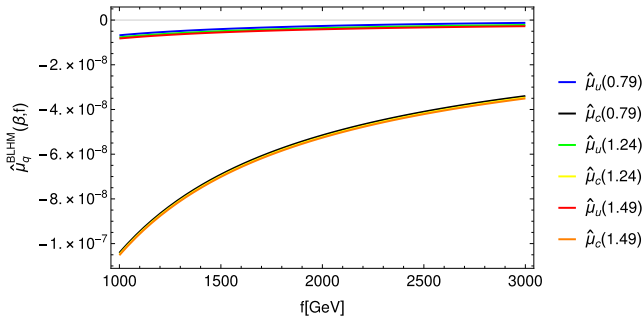


Fig. 2. (color online) Dipole of the u and c quarks in the spacelike scenario for $\beta = (0.79, 1.24, 1.49)$ radians, $1 < f < 3$ TeV, and $F = 5$ TeV. The behavior of the CMDMs as scale f increases shows the natural decoupling of $\hat{\mu}_u$ and $\hat{\mu}_c$ in the BLHM.

neutral bosons.

Figures 4 and 5 depict the dipoles of the strange and down quarks, respectively, for the same mentioned angles. They receive contributions of the order of 10^{-5} , both in spacelike and timelike configurations.

Figures 6 and 7 show the improved contributions

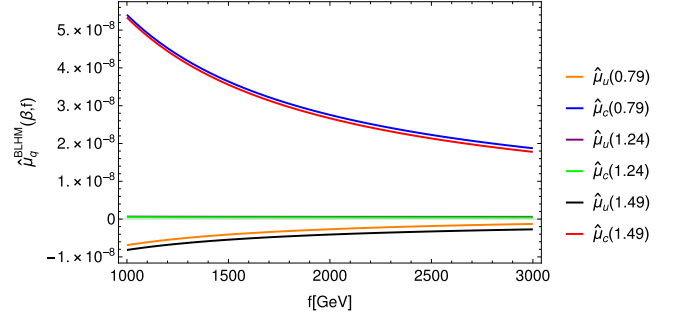


Fig. 3. (color online) Dipole of the u and c quarks in the timelike scenario with $\beta = (0.79, 1.24, 1.49)$ radians, $1 < f < 3$ TeV, and $F = 5$ TeV. As in the spacelike case, the same decoupling occurs for $\hat{\mu}_u$ and $\hat{\mu}_c$ as f increases.

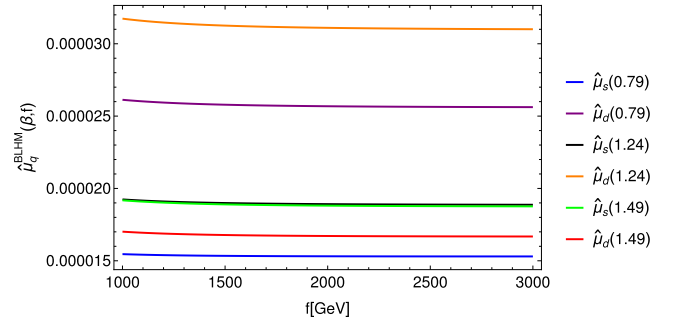


Fig. 4. (color online) Dipole of the s and d quarks in the spacelike scenario with $\beta = (0.79, 1.24, 1.49)$ radians, $1 < f < 3$ TeV, and $F = 5$ TeV. In this case, although the curves are similar to the timelike version, there are differences between $\hat{\mu}_s$ and $\hat{\mu}_d$.

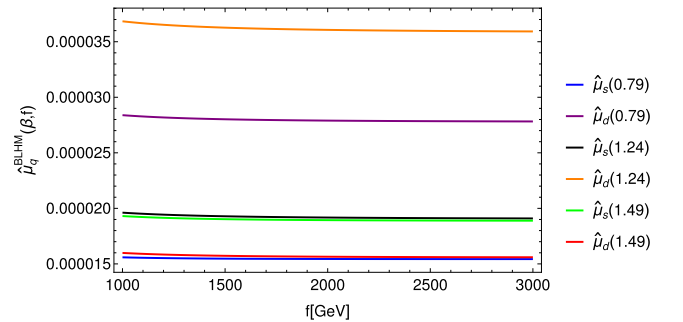


Fig. 5. (color online) Dipole of the s and d quarks in the timelike scenario with $\beta = (0.79, 1.24, 1.49)$ radians, $1 < f < 3$ TeV, and $F = 5$ TeV. In observables $\hat{\mu}_d$ and $\hat{\mu}_s$, magnitudes of the order of 10^{-5} are obtained that quickly tend toward decoupling for both schemes, $q^2 = \pm m_Z^2$.

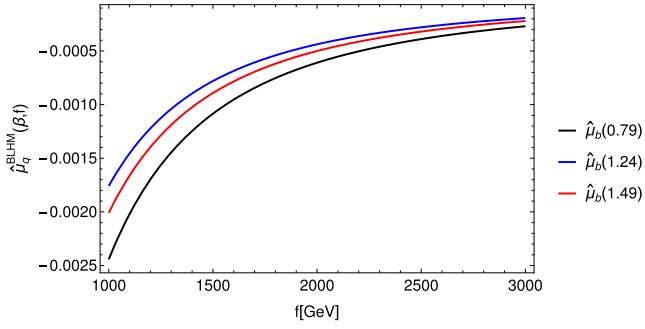


Fig. 6. (color online) Dipole of the b quark in the spacelike scenario with $\beta = (0.79, 1.24, 1.49)$ radians, $1 < f < 3$ TeV, and $F = 5$ TeV. The decoupling for $\hat{\mu}_b$ occurs in the same manner for both schemes, $q^2 = \pm m_Z^2$. However, in these cases, it occurs with a negative sign at the order of 10^{-3} , where the curves are very similar, unlike the other CMDMs, whose curves differ in shape and order from each other.

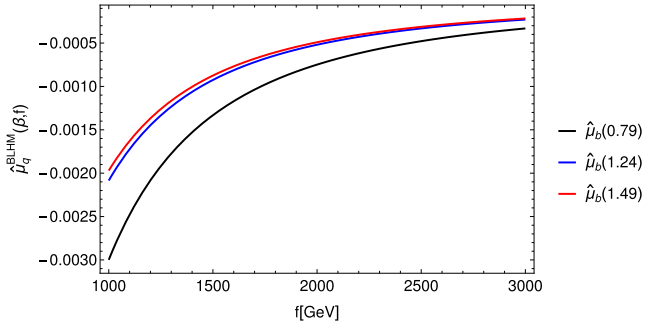


Fig. 7. (color online) Dipole of the b quark in the timelike scenario with $\beta = (0.79, 1.24, 1.49)$ radians, $1 < f < 3$ TeV, and $F = 5$ TeV. The contributions of the heavy quarks to $\hat{\mu}_b$ in both schemes, $q^2 = \pm m_Z^2$, are notable in terms of the shape of the curves.

from the BLHM quarks and bosons to the SM bottom quark. Both spacelike and timelike CMDMs are of the order of 10^{-3} . These results indicate that it is necessary to add new interactions between heavy quarks of the T type with light quarks (u, c, d, s).

In the plots shown in Figs. 2–7, differences are observed between the dipoles evaluated in the spacelike and timelike scenarios; in particular, no negative values are found in the first one. Tables 5 and 6 show that the dipoles for $f = 2$ TeV and $f = 3$ TeV do exhibit differences with respect to the $f = 1$ case, as presented in Tables 7–10. We must clarify that we have not included the imaginary parts of the CMDMs because their magnitudes are generally of the order of 10^{-20} . We have included the CMDMs of the light quarks calculated in the SM (see Table 11; note that we have not included their imaginary parts either). If we compare them with those of Tables 5 and 6, only $\hat{\mu}_c^{\text{BLHM}}$ is lower than its counterpart in the SM. By contrast, $\hat{\mu}_b^{\text{BLHM}}$ exceeds the order of $\hat{\mu}_b^{\text{SM}}$. According to the charm mass, one might expect the con-

Table 5. Numerical values for $\hat{\mu}_{q_i}^{\text{BLHM}}(\beta, f)$ spacelike at $f = 1$ TeV and $F = 5$ TeV.

β	0.79	1.24	1.49
$\hat{\mu}_u^{\text{BLHM}}$	-6.80×10^{-9}	-7.71×10^{-9}	-8.23×10^{-9}
$\hat{\mu}_c^{\text{BLHM}}$	-1.04×10^{-7}	-1.04×10^{-7}	-1.05×10^{-7}
$\hat{\mu}_s^{\text{BLHM}}$	1.54×10^{-5}	1.92×10^{-5}	1.91×10^{-5}
$\hat{\mu}_d^{\text{BLHM}}$	2.61×10^{-5}	3.17×10^{-5}	1.7×10^{-5}
$\hat{\mu}_b^{\text{BLHM}}$	-2.44×10^{-3}	-1.75×10^{-3}	-2.01×10^{-3}

Table 6. Numerical values for $\hat{\mu}_{q_i}^{\text{BLHM}}(\beta, f)$ timelike at $f = 1$ TeV and $F = 5$ TeV.

β	0.79	1.24	1.49
$\hat{\mu}_u^{\text{BLHM}}$	-6.89×10^{-9}	6.45×10^{-10}	-8.16×10^{-9}
$\hat{\mu}_c^{\text{BLHM}}$	5.4×10^{-8}	5.14×10^{-10}	5.33×10^{-8}
$\hat{\mu}_s^{\text{BLHM}}$	1.55×10^{-5}	1.46×10^{-5}	1.93×10^{-5}
$\hat{\mu}_d^{\text{BLHM}}$	2.83×10^{-5}	3.68×10^{-5}	1.59×10^{-5}
$\hat{\mu}_b^{\text{BLHM}}$	-2.99×10^{-3}	-2.08×10^{-3}	-1.97×10^{-3}

Table 7. Numerical values for $\hat{\mu}_{q_i}^{\text{BLHM}}(\beta, f)$ spacelike at $f = 2$ TeV and $F = 5$ TeV.

β	0.79	1.24	1.49
$\hat{\mu}_u^{\text{BLHM}}$	-2.64×10^{-9}	-3.58×10^{-9}	-4.12×10^{-9}
$\hat{\mu}_c^{\text{BLHM}}$	-5.15×10^{-8}	-5.22×10^{-8}	-5.26×10^{-8}
$\hat{\mu}_s^{\text{BLHM}}$	1.53×10^{-5}	1.89×10^{-5}	1.88×10^{-5}
$\hat{\mu}_d^{\text{BLHM}}$	2.56×10^{-5}	3.11×10^{-5}	1.67×10^{-5}
$\hat{\mu}_b^{\text{BLHM}}$	-6.0×10^{-4}	-4.37×10^{-4}	-5.0×10^{-4}

Table 8. Numerical values for $\hat{\mu}_{q_i}^{\text{BLHM}}(\beta, f)$ timelike at $f = 2$ TeV and $F = 5$ TeV.

β	0.79	1.24	1.49
$\hat{\mu}_u^{\text{BLHM}}$	-2.68×10^{-9}	5.95×10^{-10}	-4.08×10^{-9}
$\hat{\mu}_c^{\text{BLHM}}$	2.75×10^{-8}	4.34×10^{-10}	2.66×10^{-8}
$\hat{\mu}_s^{\text{BLHM}}$	1.54×10^{-5}	1.91×10^{-5}	1.89×10^{-5}
$\hat{\mu}_d^{\text{BLHM}}$	2.78×10^{-5}	3.60×10^{-5}	1.56×10^{-5}
$\hat{\mu}_b^{\text{BLHM}}$	-7.48×10^{-4}	-5.19×10^{-4}	-4.9×10^{-4}

Table 9. Numerical values for $\hat{\mu}_{q_i}^{\text{BLHM}}(\beta, f)$ spacelike at $f = 3$ TeV and $F = 5$ TeV.

β	0.79	1.24	1.49
$\hat{\mu}_u^{\text{BLHM}}$	-1.25×10^{-9}	-2.20×10^{-9}	-2.74×10^{-9}
$\hat{\mu}_c^{\text{BLHM}}$	-5.15×10^{-8}	-3.46×10^{-8}	-3.50×10^{-8}
$\hat{\mu}_s^{\text{BLHM}}$	1.53×10^{-5}	1.88×10^{-5}	1.87×10^{-5}
$\hat{\mu}_d^{\text{BLHM}}$	2.56×10^{-5}	3.10×10^{-5}	1.66×10^{-5}
$\hat{\mu}_b^{\text{BLHM}}$	-6.09×10^{-4}	-1.93×10^{-4}	-2.20×10^{-4}

Table 10. Numerical values for $\hat{\mu}_{q_i}^{\text{BLHM}}(\beta, f)$ timelike at $f = 3$ TeV and $F = 5$ TeV.

β	0.79	1.24	1.49
$\hat{\mu}_u^{\text{BLHM}}$	-1.27×10^{-9}	5.86×10^{-10}	-2.71×10^{-9}
$\hat{\mu}_c^{\text{BLHM}}$	1.87×10^{-8}	4.19×10^{-10}	1.77×10^{-8}
$\hat{\mu}_s^{\text{BLHM}}$	1.54×10^{-5}	1.90×10^{-5}	1.88×10^{-5}
$\hat{\mu}_d^{\text{BLHM}}$	2.78×10^{-5}	3.59×10^{-5}	1.55×10^{-5}
$\hat{\mu}_b^{\text{BLHM}}$	-3.31×10^{-4}	-2.29×10^{-4}	-2.16×10^{-4}

Table 11. Numerical values for $\hat{\mu}_{q_i}^{\text{SM}}$ in the SM, spacelike and timelike [17].

	$q^2 = -m_Z^2$	$q^2 = m_Z^2$
$\hat{\mu}_u^{\text{SM}}$	-1.15×10^{-10}	-1.15×10^{-10}
$\hat{\mu}_c^{\text{SM}}$	-1.16×10^{-5}	1.15×10^{-5}
$\hat{\mu}_s^{\text{SM}}$	-1.38×10^{-7}	1.37×10^{-7}
$\hat{\mu}_d^{\text{SM}}$	-5.07×10^{-10}	-5.04×10^{-10}
$\hat{\mu}_b^{\text{SM}}$	-1.61×10^{-4}	1.55×10^{-4}

tributions to the dipole to be of a magnitude close to that of the bottom; however, they turned out to be very small. This means that the contributions of the quarks ($T, T^5, T^6, T^{2/3}$) are much more significant than those of all the heavy bosons because the order of $\hat{\mu}_b^{\text{BLHM}}$ is much higher owing to the heavy up-type quarks.

VI. CONCLUSIONS

We calculated the dipoles of light quarks of the SM (u, c, d, s, b) with contributions from heavy quarks and bosons of the BLHM, as well as bosons (h^0, Z, γ, W^\pm) of the SM, both in the spacelike ($q^2 = -m_Z^2$) and timelike ($q^2 = m_Z^2$) scenarios. We found that the magnitudes of our results are greater than similar ones in the SM. The dipole for which we obtained the largest contributions from the BLHM is the CMDM of the bottom quark, $O(10^{-3})$, which receives contributions from all heavy quarks and bosons. By contrast, the dipoles of the other light quarks (u, c, d, s) only receive contributions from heavy quark B and heavy bosons [19], as can be observed from the Feynman rules in Tables 12 and 13. Accordingly, we conclude that it is also necessary to extend interactions of the heavy up-type quarks to all four light quarks (u, c, d, s). In this study, we also used extended CKM matrices V_{Hu} and V_{Hd} , parameterizing only one case of them in relation to the V_{CKM} matrix. The elements of the extended matrices further constrained dipoles $\hat{\mu}_{q_i}$ in comparison with the dipoles calculated for the top quark in [27], as in the BLHM. The magnitudes of the CMDMs calculated in the BLHM, mainly for the bottom quark, encourage us to expect new experimental signals that may provide hints of

Table 12. Essential Feynman rules in the BLHM to study the CMDM of light quarks are the 3-point interactions fermion-fermion-scalar (FFS) and fermion-fermion-gauge (FFV) interactions.

Vertex	Rule
$W'^- \bar{B}u$	$\frac{ig g_A}{2\sqrt{2}g_B} \gamma^\mu P_L (V_{Hu})$
$W'^- \bar{B}c$	$\frac{ig g_A}{2\sqrt{2}g_B} \gamma^\mu P_L (V_{Hu})$
$\eta^- \bar{B}u$	$-\frac{im_B s_\beta^2}{2f\sqrt{2}} P_L (V_{Hu})$
$\eta^- \bar{B}c$	$-\frac{m_B s_\beta^2}{2f\sqrt{2}} P_L (V_{Hu})$
$\eta^0 \bar{B}d$	$-\frac{im_B s_\beta^2}{4f} P_L$
$\eta^0 \bar{B}s$	$-\frac{im_B s_\beta^2}{4f} P_L$
$\phi^- \bar{B}u$	$\frac{iF s_\beta^2 [m_u + m_B + (m_u - m_B)\gamma^5]}{2f\sqrt{2}\sqrt{f^2 + F^2}} (V_{Hu})$
$\phi^- \bar{B}c$	$\frac{iF s_\beta^2 [m_c + m_B + (m_c - m_B)\gamma^5]}{2f\sqrt{2}\sqrt{f^2 + F^2}} (V_{Hu})$
$\phi^0 \bar{B}d$	$\frac{iF m_B s_\beta^2}{4f\sqrt{f^2 + F^2}} P_L$
$\phi^0 \bar{B}s$	$\frac{iF m_B s_\beta^2}{4f\sqrt{f^2 + F^2}} P_L$
$H^- \bar{B}u$	$\frac{g m_B s_\beta^2}{4\sqrt{2}m_W} P_L (V_{Hu})$
$H^- \bar{B}c$	$\frac{g m_B s_\beta^2}{4\sqrt{2}m_W} P_L (V_{Hu})$
$H^0 \bar{B}d$	$-\frac{g m_B s_\alpha s_\beta}{4m_W} P_L$
$H^0 \bar{B}s$	$-\frac{g m_B s_\alpha s_\beta}{4m_W} P_L$

Table 13. Essential Feynman rules in the BLHM to study the CMDM of light quarks are the 3-point interactions fermion-fermion-scalar (FFS) and fermion-fermion-gauge (FFV) interactions.

Vertex	Rule
$h^0 \bar{B}d$	$\frac{g m_B c_\alpha s_\beta}{4m_W} P_L$
$h^0 \bar{B}s$	$\frac{g m_B c_\alpha s_\beta}{4m_W} P_L$
$A^0 \bar{B}d$	$-\frac{g m_B s_\beta^2}{8m_W} P_L$
$A^0 \bar{B}s$	$-\frac{g m_B s_\beta^2}{8m_W} P_L$
$\sigma \bar{B}d$	$\frac{m_B s_\beta^2}{4\sqrt{2}m_W f} P_L$
$\sigma \bar{B}s$	$\frac{m_B s_\beta^2}{4\sqrt{2}m_W f} P_L$
$Z \bar{B}d$	$-\frac{ig'^2 s_W}{4g'} \gamma^\mu P_L$
$Z \bar{B}s$	$-\frac{ig'^2 s_W}{4g'} \gamma^\mu P_L$

Continued on next page

Table 13-continued from previous page

Vertex	Rule
$Z'\bar{b}d$	$-\frac{ig_{GA}}{4g_B}\gamma^\mu P_L$
$Z'\bar{b}s$	$-\frac{ig_{GA}}{4g_B}\gamma^\mu P_L$
$\gamma\bar{b}d$	$-\frac{ig_{SW}}{4}\gamma^\mu$
$\gamma\bar{b}s$	$-\frac{ig_{SW}}{4}\gamma^\mu$

new physics. It is important to remember that the CMDMs or CEDMs of light quarks have not been evaluated in other BSM models as we did in this study. We hope that this will be eventually done to enrich our own work on this topic.

References

- [1] R. Martinez and J. A. Rodriguez, *Phys. Rev. D* **55**, 3212 (1997)
- [2] R. Martinez and J. A. Rodriguez, *Phys. Rev. D* **65**, 057301 (2002)
- [3] R. Martinez, M. A. Perez, and N. Poveda, *Eur. Phys. J. C* **53**, 221 (2008)
- [4] D. Buarque Franzosi and C. Zhang, *Phys. Rev. D* **91**, 114010 (2015)
- [5] J. I. Aranda, T. Cisneros-Pérez, J. Montaña *et al.*, *Eur. Phys. J. Plus* **136**, 164 (2021)
- [6] G. Aad *et al.* (ATLAS), *JHEP* **06**, 145 (2021)
- [7] L. Ding and C. X. Yue, *Commun. Theor. Phys.* **50**, 441 (2008)
- [8] A. I. Hernández-Juárez, A. Moyotl, and G. Tavares-Velasco, *Phys. Rev. D* **98**, 035040 (2018)
- [9] A. I. Hernández-Juárez, G. Tavares-Velasco, and A. Moyotl, *Chin. Phys. C* **45**, 113101 (2021)
- [10] J. I. Aranda, T. Cisneros-Pérez, E. Cruz-Albaro *et al.*, arXiv: 2111.03180 [hep-ph]
- [11] S. Rappoccio, *Rev. Phys.* **4**, 100027 (2019)
- [12] E. Cruz-Albaro and A. Gutiérrez-Rodríguez, *Eur. Phys. J. Plus* **137**, 1295 (2022)
- [13] E. Cruz-Albaro, A. Gutiérrez-Rodríguez, J. I. Aranda *et al.*, *Eur. Phys. J. C* **82**, 1095 (2022)
- [14] E. Cruz-Albaro, A. Gutiérrez-Rodríguez, M. A. Hernandez-Ruiz *et al.*, *Eur. Phys. J. Plus* **138**, 506 (2023)
- [15] I. D. Choudhury and A. Lahiri, *Mod. Phys. Lett. A* **30**, 1550113 (2015)
- [16] A. I. Hernández-Juárez, A. Moyotl, and G. Tavares-Velasco, *Eur. Phys. J. Plus* **136**, 262 (2021)
- [17] J. Montano-Dominguez, B. Quezadas-Vivian, F. Ramirez-Zavaleta *et al.*, *Int. J. Mod. Phys. A* **38**, 2350071 (2023)
- [18] W. Bernreuther and Z. G. Si, *Phys. Lett. B* **725**, 115 (1965), [Erratum: *Phys. Lett. B* **744**, 413 (2015)]
- [19] T. Cisneros-Pérez, M. A. Hernández-Ruiz, A. Gutiérrez-Rodríguez *et al.*, *Eur. Phys. J. C* **83**, 1093 (2023)
- [20] M. Schmaltz, D. Stolarski, and J. Thaler, *JHEP* **09**, 018 (2010)
- [21] M. Schmaltz and J. Thaler, *JHEP* **03**, 137 (2009)
- [22] K. Moats, arXiv: 2403.08021 [hep-ph]
- [23] M. Kobayashi and T. Maskawa, *Prog. Theor. Phys.* **49**, 652 (1973)
- [24] T. A. W. Martin, *Examining extra neutral gauge bosons in non-universal models and exploring the phenomenology of the Bestest Little Higgs model at the LHC*, Doctoral thesis (Carleton University, 2012)
- [25] S. Godfrey, T. Gregoire, P. Kalyniak *et al.*, *JHEP* **04**, 032 (2012)
- [26] P. Kalyniak, T. Martin, and K. Moats, *Phys. Rev. D* **91**, 013010 (2015)
- [27] T. Cisneros-Pérez, M. A. Hernández-Ruiz, A. Ramirez-Morales *et al.*, arXiv: 2403.08021 [hep-ph]
- [28] A. Tumasyan *et al.* (CMS), *JHEP* **12**, 161 (2021)
- [29] A. M. Sirunyan *et al.* (CMS), *Phys. Lett. B* **805**, 135425 (2020)
- [30] N. Hashemi and M. Ghalati, *Phys. Lett. B* **830**, 137153 (2022)
- [31] G. Aad *et al.* (ATLAS), *Eur. Phys. J. C* **81**, 396 (2021)
- [32] G. Aad *et al.* (ATLAS Collaboration), *Phys. Lett. B* **744**, 163 (2015)
- [33] A. M. Sirunyan *et al.* (CMS Collaboration), *JHEP* **03**, 055 (2020)
- [34] M. Hashemi and G. Haghghat, *Eur. Phys. J. C* **79**, 419 (2019)
- [35] A. Tumasyan *et al.* (CMS Collaboration), *JHEP* **09**, 032 (2023)
- [36] J. Wells, *Phys. Rev. D* **107**, 055022 (2023)
- [37] D. Buttazzo, A. Greljo, and D. Marzocca, *Eur. Phys. J. C* **76**, 116 (2016)
- [38] U. Haisch, G. Polesello, and S. Schulte, *JHEP* **09**, 206 (2021)
- [39] G. Aad *et al.* (ATLAS Collaboration), *JHEP* **08**, 153 (2023)
- [40] G. Aad *et al.* (ATLAS Collaboration), *Eur. Phys. J. C* **83**, 719 (2023)
- [41] M. Aaboud *et al.* (ATLAS), *JHEP* **07**, 089 (2018)
- [42] A. M. Sirunyan *et al.* (CMS), *JHEP* **08**, 177 (2018)
- [43] A. Tumasyan *et al.* (CMS), *JHEP* **09**, 051 (2023)
- [44] A. Tumasyan *et al.* (CMS), *Phys. Rev. D* **105**, 032008 (2022)
- [45] A. M. Sirunyan *et al.* (CMS), *Eur. Phys. J. C* **81**, 688 (2021)
- [46] V. Shtabovenko, R. Mertig, and F. Orellana, *Comput. Phys. Commun.* **256**, 107478 (2020)
- [47] H. H. Patel, *Comput. Phys. Commun.* **218**, 66 (2017)
- [48] M. Blanke, A. J. Buras, A. Poschenrieder *et al.*, *Phys. Lett. B* **646**, 253 (2007)
- [49] M. Blanke, A. J. Buras, A. Poschenrieder *et al.*, *JHEP* **01**, 066 (2007)

ACKNOWLEDGMENTS

T. C. P. and E. C. A. thanks SNII and CONAHCYT (México) postdoctoral fellowships.

APPENDIX A: FEYNMAN RULES IN THE BLHM

In this appendix, we derive and present the Feynman rules for the BLHM necessary to calculate the CMDM of light quarks. The Feynman rules for the b quark and other fields can be found in references [10, 14, 19].

Tables 12 and 13 summarize the Feynman rules for the 3-point interactions: fermion-fermion-scalar (FFS) and fermion-fermion-gauge (FFV) interactions.